Degradable melamine-based adhesives using dynamic silyl ether bonds

*Ian C. Pierce※, Jorge Barroso ,†, Joanne B. Ko※, Bess Vlaisavljevich , Julia A. Kalow※**

※Department of Chemistry, Northwestern University, Evanston, Illinois 60208, United States

§Department of Chemistry, The University of South Dakota, Vermillion, South Dakota 57069, United States

†Department of Chemistry, Clemson University, Clemson, South Carolina 29634, United States

Abstract

Materials made from covalently crosslinked polymer networks are ubiquitous in everyday life but are difficult to process at the end of their life cycle. Materials designed with sustainability in mind will play a critical role in reducing the detrimental effects of plastic waste build-up. Functionalized triazines such as 1,3,5-triazine-2,4,6-triamine (melamine), hexamethylol melamine (HMM), and hexa(methoxymethyl)melamine (HMMM) are key components of robust thermosets, adhesives, and coatings. We combine HMM and HMMM with an alkoxysilane to produce transparent thermosets with remarkable glass adhesion. The dynamicity of silyl ether bonds in the network makes the materials susceptible to methanolysis, enabling the recovery of HMMM and the substrate. A combination of solution- and solid-phase techniques are used to elucidate both gelation and degradation pathways.

Keywords

Degradation, melamine, thermoset, dynamic, network, adhesive, silyl ether

1. Introduction

Thermoset materials are valued for their durability in a broad range of applications. The permanent crosslinks holding these polymer systems together create networks resistant to physical or chemical changes. These materials are used as coatings, adhesives, composites, and standalone resins with a growing global production exceeding 50 million tons.[1,2] Triazine-based crosslinkers such as melamine (Figure 1a) are frequently used for rigid, thermally stable products thanks to the aromatic core.[3–5] Melamine has been used in crosslinked polyureas, dinnerware, wood binders, and substrate coatings.[6–10] When heated, or in sufficiently acidic or alkaline environments, the combination of melamine and formaldehyde forms a network of ether and methylene linkages.[11] Hexamethylol melamine (HMM) has been noted as an important intermediate in the formation of these networks[12] and many additional alkoxy derivatives, such as hexa(methoxymethyl)melamine (HMMM), can be readily derived from HMM.[13] These triazines are used as crosslinkers and are common additives to enhance the flame retardancy of various polymers.[14–18]

The permanent covalent bonds between polymer strands that endow thermosets with robust physical and chemical properties also make these networks difficult to recycle or degrade. However, when the permanent crosslinks are replaced with dynamic bonds, molecular rearrangement can occur with appropriate thermal or chemical stimuli.[19] Silyl ether dynamic bonds are attractive for the degradation and recycling of polymers due to their ease of incorporation and tunability.[20–22] While observations of bond exchange in polydimethylsiloxane (PDMS) date back to the 1950s,[23,24] recent work has expanded the possibilities for silyl ether materials using both exchange and metathesis pathways, which can be internally or externally catalyzed (Figure 1b).[25–27] We hypothesized that alkoxysilanes could be combined with the free hydroxy groups in HMM to afford dynamic triazine networks that are more sustainable than existing resins (Figure 1c).

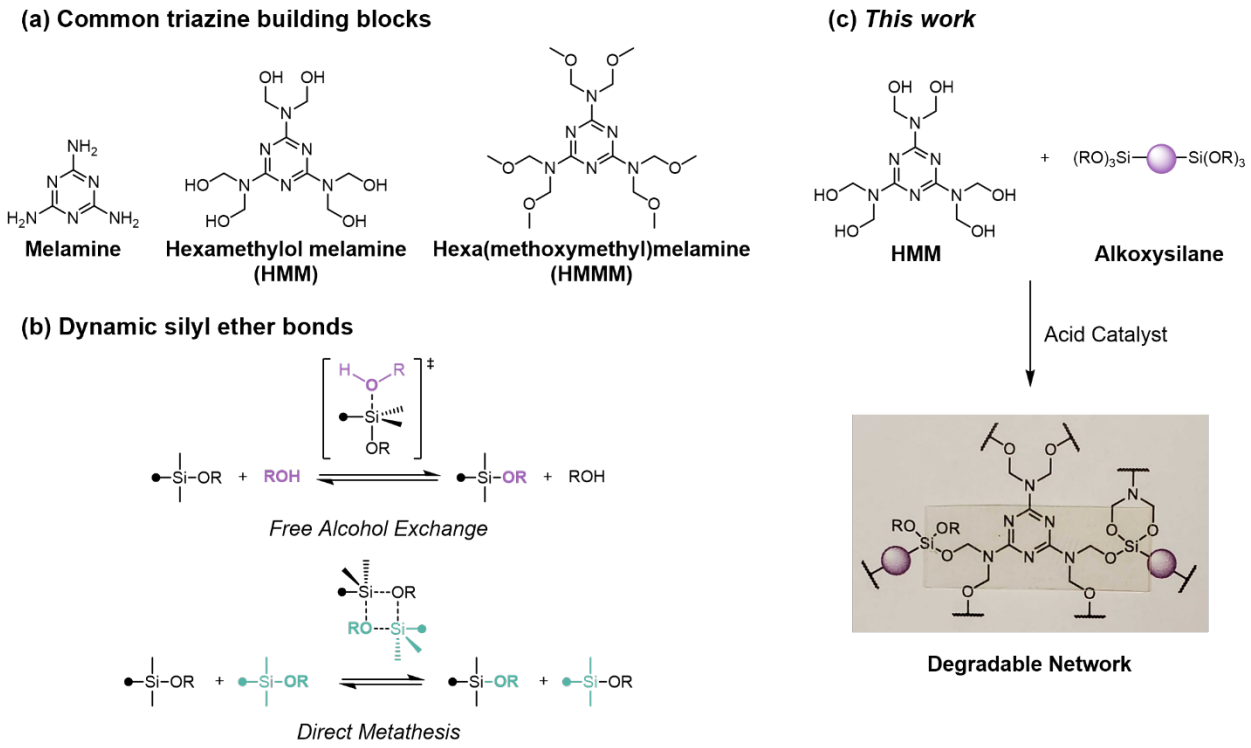

Figure 1. (a) Triazines commonly used in thermoset materials. (b) Mechanisms of bond exchange in silyl ethers. (c) Components of our network with a representative sample overlaid on the proposed network structure.

The combination of triazine materials and alkoxysilanes has been reported in niche applications, including non-linear optics, but there has been no exploration of bond exchange within these materials.[28–30] In fact, reprocessable materials based on triazine compounds are largely unexplored. The only examples of reprocessable and degradable melamine materials are recent publications by Urdl and coworkers using the Diels-Alder reaction[31–33] and by Zhang and coworkers using nucleophilic aromatic substitution.[34] Here, we describe the preparation of triazine-containing silyl ether networks and their applications as degradable adhesives and coatings.

2. Experimental

2.1 Materials

Reagents and solvents were purchased from TCI, MilliporeSigma, Acros, Fisher Scientific, and Cambridge Isotope Laboratories and used without further purification. Deionized water was used exclusively in preparation and workups. 1,4-Bis(trimethoxysilylethyl)benzene (BTMSEB) was purchased from Gelest. pH was estimated using Fishebrand™ plastic pH strips with a pH range of 0–14. Glass slides were provided by McMaster-Carr (1 x 3 x 0.125 in.) or by Fisher Scientific (25 x 75 x 1 mm). Additional details can be found in the Supporting Information (SI).

2.2 Preparation of HMM

1,3,5-triazine-2,4,6-triamine (5.00 g, 39.6 mmol) was suspended in 10 mL of water in a 100 mL round-bottom flask equipped with a stir bar. While heating to 65 °C in an oil bath, a formaldehyde solution was prepared by slowly adding 1M NaOH to 37 wt.% formaldehyde in water (7 eq., 20.7 mL, 278 mmol) until the pH reached 9. The formaldehyde solution was added dropwise while stirring, the reaction was held at 65 °C for 2 hours, then removed from the heat and cooled for 1 hour. The resulting white slurry was vacuum filtered and rinsed with 500 mL of cold water and dried. Additional preparations and characterization are provided in the SI.

2.3 Preparation of networks

HMM-net samples were prepared using a 0.65 M solution of HMM dispersed in tetrahydrofuran (THF) with 10 mol% *p*-toluenesulfonic acid monohydrate (PTSA) and 2 equivalents of BTMSEB. After everything was well combined, the mixture was heated to 50 °C with constant stirring until the solution began to clear after 10 minutes. Solutions were degassed before transferring to molds or glass slides.

HMMM-net samples were prepared using a 1.6 M solution of HMMM dissolved in THF. This was diluted with 33 vol.% water containing 10 mol% PTSA followed by the addition of 2

equivalents of BTMSEB. The solution was mixed vigorously for 30 seconds, degassed, and transferred to molds or glass slides.

For films, the molds were held under reduced pressure at 23 °C until gelation occurred and the materials were no longer tacky (16 hours for HMM-net and 10 minutes for HMMM-net). Any desired trimming was performed at this point when the materials were still flexible. This was followed by a final cure in a vacuum oven at 90 °C for 2 hours to produce clear, brittle films.

Adhesive samples were prepared by transferring 50 μL of the degassed liquid to a 1 x 1 in. area of a glass slide precleaned with acetone. Samples were immediately clamped and cured at 90 °C for 2 hours under reduced pressure. Commercial adhesive samples were prepared according to the manufacturer's label. Additional details regarding sample preparation are located in the SI.

2.4 Adhesion testing

Glass slides were secured in an MTS Criterion universal test system with a 100 kN load cell using offset manual vise grips 0.5 inches from the sample area. The upper grip was moved at a rate of 0.6 mm/s until failure and the type of failure was recorded. The maximum force was used to determine the shear strength of the adhesive. Full procedures and results can be found in the SI.

Degradation of networks

Pieces of HMM-net (50-100 mg) were placed in a pressure vessel and submerged in 10 mL of methanol. The sealed vessel was brought to 90 °C in an oil bath and held at temperature for between 30 minutes and 6 days. The contents of the vessel were vacuum filtered and washed with 10 mL of methanol. The methanol fraction was collected and concentrated under reduced pressure, then both the sol fraction and gel fraction were dried overnight. Additional procedures can be found in the SI.

2.5 Instrumentation

Proton (^{1}H) and carbon (^{13}C) nuclear magnetic resonance (NMR) spectra were measured on Bruker AVANCE-500 spectrometers at 500 MHz and 125 MHz, respectively, and referenced to the residual solvent peak. A Bruker AVANCE HD Nanobay with BBFO probe was used to collect ^{1}H NMR spectra at 400 MHz and automated intervals for reaction monitoring. Infrared spectroscopy (IR) was performed at room temperature on a Bruker Tensor 37 FTIR Spectrometer. Transmittance of the coatings on Fisher Scientific microscope slides was measured on a Perkin Elmer LAMBDA 1050 UV/Vis/NIR double beam spectrophotometer. Small-amplitude oscillatory shear (SAOS) experiments were performed on a TA Instruments DHR-30 rheometer with a 25 mm diameter parallel plate geometry. Single lap shear adhesion tests were performed on an MTS Criterion universal test system. Thermogravimetric analysis (TGA) was performed under nitrogen on a TA TGA5500 instrument at a ramp rate of 10 °C/min. Differential scanning calorimetry (DSC) was performed under nitrogen on a TA Instruments DSC-250 at a ramp rate of 5 °C/min. X-Ray photoelectron spectroscopy (XPS) was performed on a ThermoFisher Scientific NEXSA G2 spectrometer. Further specifications and details regarding sample preparation can be found in the SI.

3. Results and Discussion

3.1 Monomer Selection and Reactivity

3.1.1 Network Formation

By controlling the temperature and acidity of the reaction between melamine and formaldehyde, HMM can be isolated without further conversion to a crosslinked network.[11] Based on previous reports using silyl ethers in dynamic networks,[25,26] we hypothesized that HMM could serve as a polyol to condense with a multifunctional silyl ether. We selected commercially available 1,4-bis(trimethoxysilylethyl)benzene (BTMSEB, Figure 2a) as the alkoxysilane crosslinker, predicting

that the aromatic core would help maintain the desirable properties of melamine-formaldehyde resins.

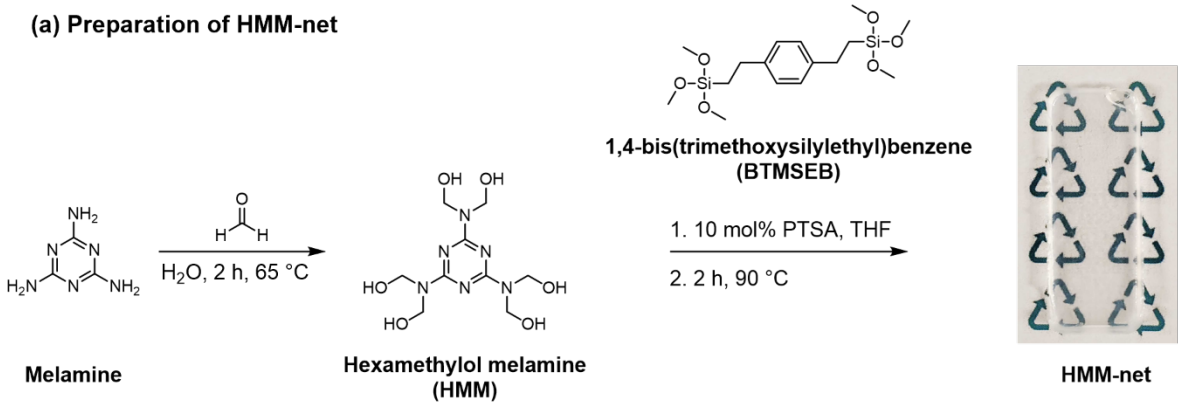

(b) Gel fractions of HMM-net

Solvent	Gel fraction (%)
Acetonitrile	>99
Dimethyl sulfoxide	>99
Ethyl Acetate	>99
Methanol	>98
Toluene	>99
Water	>99

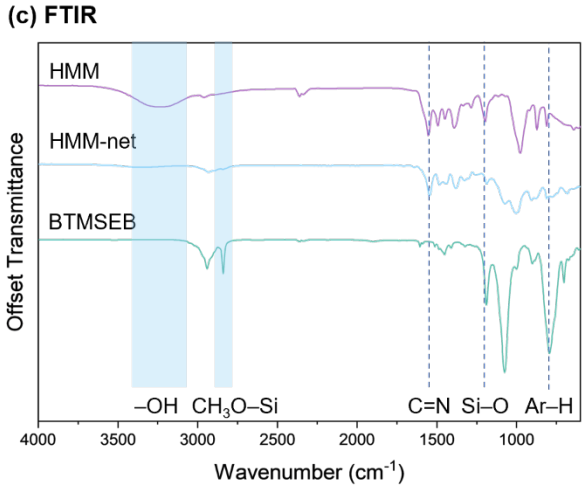

Figure 2. (a) Synthetic scheme starting from melamine, showing the formation of HMM-net as a clear, free-standing network. (b) Gel fractions of HMM-net recorded after soaking in various solvents for 72 hours at 23 ºC. (c) FTIR of the reaction stages with peaks consumed during the reaction highlighted in blue and dashed lines indicating the peaks from the starting materials that can be identified in the final network.

To minimize self-condensation[35,36] and promote silyl ether formation between HMM and BTMSEB, we attempted to combine the reagents in tetrahydrofuran (THF) without a catalyst. However, gelation did not occur and HMM remained insoluble. *Para*-toluenesulfonic acid (PTSA)

was thus selected as an acid catalyst to promote condensation based on prior uses with melamine and alkoxysilanes.[30] While HMM is insoluble in THF, adding acid catalyst caused the cloudy solution to turn clear as HMM reacted with the BTMSEB, corresponding with a sharp increase in viscosity followed by gelation. As a control, HMM was combined with PTSA in THF at 23 °C and did not produce a gel. Likewise, BTMSEB in a THF/PTSA solution remained a stable liquid for over a week, showing that neither component forms a network alone (see SI).

The clear HMM/BTMSEB solutions were transferred to molds, cured under reduced pressure to remove excess solvent, and annealed at 90 °C to produce a clear, brittle film. Gel fractions in various solvents were consistently greater than 95%, demonstrating a high degree of crosslinking and solvent resistance (Figure 2b). Fourier transform infrared (FTIR) spectroscopic analysis of the film showed near complete consumption of hydroxy groups from HMM (3233 cm^{-1}) and the sharp methoxy peak of BTMSEB (2839 cm^{-1}). Notably, the networks still exhibited peaks associated with the triazine (1553 cm^{-1}), Si–O (1075 cm^{-1}), and benzene C–H (794 cm^{-1}) indicating that all starting materials were incorporated into the system as expected (Figure 2c).[37,38]

3.1.2 Mechanism of Condensation

We next evaluated gelation with several common Lewis and Brønsted acid catalysts. Two Lewis acid catalysts, zinc (II) triflate and scandium (III) triflate ($Zn(OTf)_2$ and $Sc(OTf)_3$, respectively), and a Brønsted acid catalyst, camphorsulfonic acid (CSA), were selected for comparison to PTSA based on previous reports.[26] Solutions of HMM in DMSO-d_6 (0.05 M) were prepared with dimethyl sulfone as an internal standard. After 10 mol% of the acid was thoroughly incorporated, 2 equivalents of BTMSEB relative to HMM were added. NMR spectra were collected every minute for 30 minutes at various temperatures (Figures S8-14). The most striking change was the rapid production of methanol (MeOH) at 3.17 ppm, which was used to track the progress and efficiency

of the reaction. The formation of methanol was closely associated with changes in the peaks from BTMSEB, mainly the peak corresponding to the methoxy group of the alkoxysilane. This peak (3.46 ppm) rapidly disappears as the methanol concentration increases (Figure 3a). Different degrees of OH substitution of the Si center caused distinct shifts in the methylene peaks nearest the silicon atom of BTMSEB as the alkoxysilane is hydrolyzed to form silanol. The other BTMSEB peaks could not be deconvoluted, but the aromatic region maintained a constant concentration relative to the internal standard indicating that both alkoxysilane and silanol remained in solution. The methylene peak at 5.01 ppm corresponding to HMM showed some broadening and a slight decrease in concentration. This decrease could be attributed to oligomerization of HMM that would affect solubility. We were able to assign the broadening of the peak to the formation of HMMM, which has a methylene peak that overlaps with HMM. The presence of HMMM suggests that free methanol from the hydrolysis of BTMSEB can replace the hydroxy of HMM. Consumption of methanol through this pathway could explain why the final concentration of methanol does not match the amount expected from full BTMSEB hydrolysis. The hydrolysis of BTMSEB proceeded quickly in all cases, plateauing in under 30 minutes at 50 °C for all catalysts except $Zn(OTf)_2$ (Figure 3b). Only $Sc(OTf)_3$ performed similarly to PTSA, but given the lower cost of the Brønsted acid, PTSA is the preferred catalyst for applications of these materials.

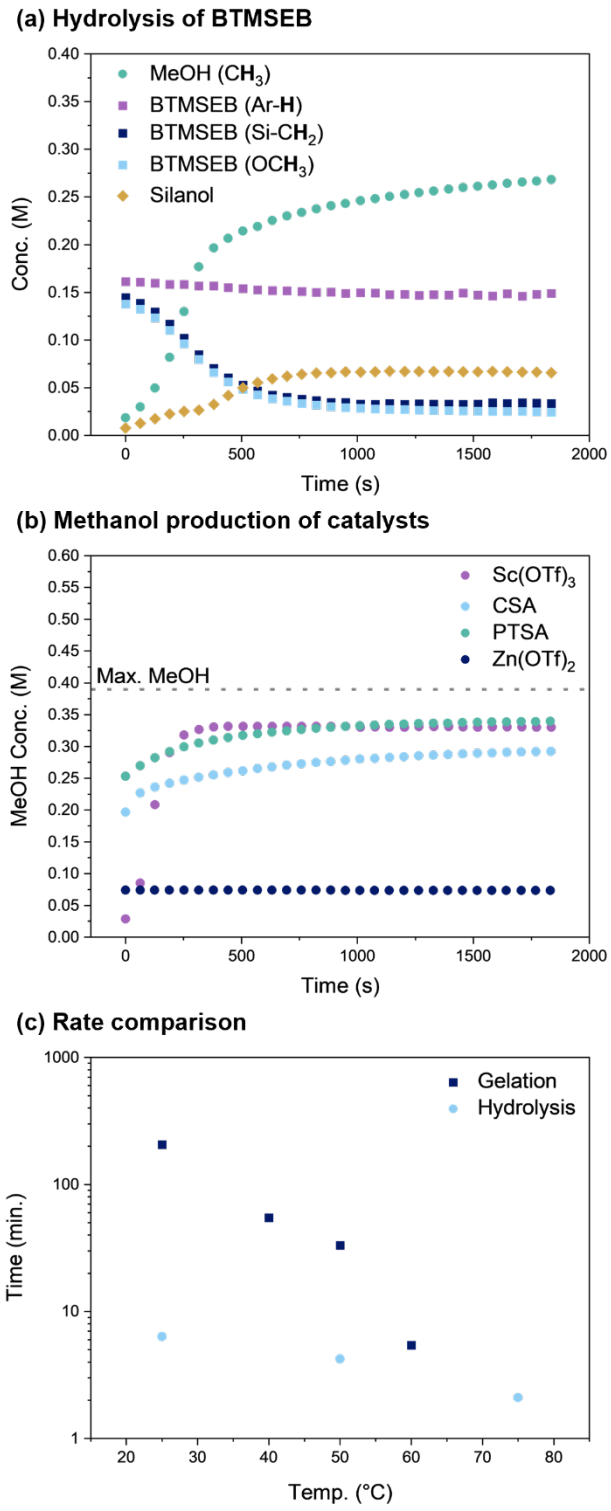

Figure 3. (a) Change in concentration of starting materials based on NMR during BTMSEB hydrolysis with $Sc(OTf)_3$ at 25 °C. (b) Methanol evolution for various catalysts at 50 °C. (c) The

time to gelation, based on crossover point by SAOS, and time to BTMSEB hydrolysis, based on MeOH formation reaching a plateau, at different temperatures.

While designing our network, we initially hypothesized that the hydroxyl group of HMM would act as a nucleophile, attacking the BTMSEB silicon and releasing methanol (Scheme 1a). While the methanol evolution observed by NMR results seemed to corroborate this hypothesis, we could only gain insight into soluble (non-network) species using this method. Therefore, we used small-amplitude oscillatory shear (SAOS) rheology measurements to track the critical gel point, the crossover point between the storage and loss moduli, over time (Figure S16). These rheological experiments showed gelation occurred on a much longer timescale than MeOH generation, even though the rheological experiments were performed at higher concentration (0.22 M). For example, when using $Sc(OTf)_3$ as the catalyst, hydrolysis of BTMSEB was complete within 5 minutes at 25 °C by NMR, but the gel point only occurred after nearly 3.5 hours (Figure 3c). Increasing temperature sped up the gelation, but it still lagged significantly behind hydrolysis of BTMSEB. The fact that the system remains a liquid until high conversion of starting material is consistent with a step-growth mechanism. Nevertheless, we considered alternative mechanisms for network formation that could account for our observations.

Scheme 1. (a) The originally hypothesized mechanism with HMM acting as the nucleophile and (b) the updated hypothesis involving the formation of an iminium ion and silanol.

(a) Initial mechanistic hypothesis

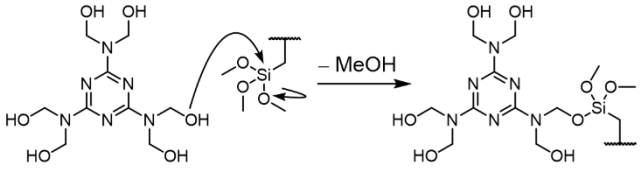

(b) Proposed mechanism

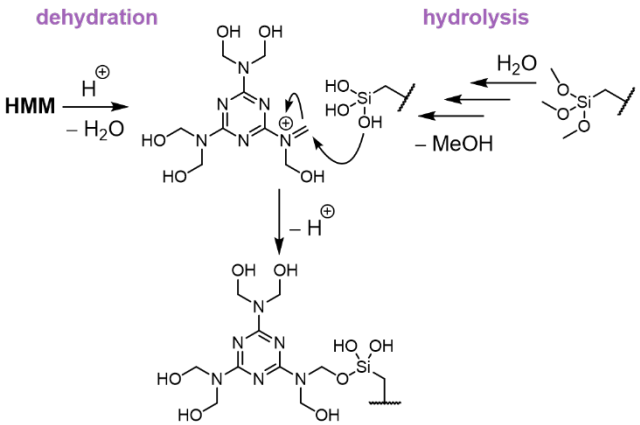

Since we observed the formation of HMMM in the NMR experiments, we evaluated its viability as an intermediate by making films from HMMM and BTMSEB. Gratifyingly, films could be formed using the same alkoxysilane and catalyst, but additional water was required for complete conversion. When HMMM was directly substituted for HMM in our formulations, no gelation was observed in a sealed reaction vessel. However, leaving the vessels uncapped showed at least partial gelation, suggesting adventitious water from the air is required. We then adjusted the formulation with HMMM to include water (33 v/v%) and achieved rapid gelation even in sealed containers. In fact, the gelation of HMMM in the presence of water occurred faster than the gelation of HMM under standard conditions. Despite these differences, the networks appeared chemically similar by FTIR, so both formulations were adopted for sample production (Figure S1).

We hypothesize that network formation in fact occurs via silanol attack on iminium derived from HMM or HMMM (Scheme 1b). Using HMM as the starting material, acid-catalyzed dehydration produces the electrophile and generates water. The water rapidly hydrolyzes BTMSEB, resulting

in the formation of MeOH observed by ^{1}H NMR and a proposed silanol intermediate. The iminium either reacts with MeOH, which can ultimately produce HMMM, or with silanol, which generates the silyl ether network. Consistent with this hypothesis, in the absence of water, HMMM, BTMSEB, and PTSA undergo no reaction up to 115 ºC (Figure S15). When 75 μL of water (30 vol.%) is added, BTMSEB is consumed and methanol is produced at 25 °C. Thus, HMMM is not a direct intermediate in the formation of our networks, but rather the product of a reversible side reaction of HMM with methanol.

To provide computational support for the proposed mechanism, we calculated DFT-derived Fukui functions of proposed reactants to determine their potential reactive sites (Figure S17).[39,40] Fukui functions are local reactivity descriptors that emerge from conceptual DFT. Specifically, the nucleophilic susceptible regions of the hydrolyzed BTMSEB, HMM, and dehydrated HMM (iminium) were determined by subtracting the electron density of the related anion from the neutral one. Similarly, the electrophilic sites were characterized by subtracting the electron density of the neutral system from that of the cation. The differences in electron density showed the electrophilic region of silanol is centered on the benzene ring, which is unlikely to be a reactive site, but reveals a significant nucleophilic region in the silanol groups of the hydrolyzed BTMSEB. Although HMM is thermodynamically stable, removing water to form an iminium ion provides a good electrophile. Therefore, we propose that ethers most likely form through attack of the silanol nucleophiles on the HMM-derived iminium electrophiles.

3.2 Adhesive Properties

Since silanol is a proposed intermediate in the formation of our networks, we explored our materials as adhesives for glass. We hypothesized that our network could chemically crosslink with free silanol on the glass surface, enabling strong adhesion. Solutions of HMM or HMMM,

BTMSEB, and PTSA in THF were applied to overlapping 1/8-inch-thick glass slides and cured at 90 °C for 2 h with clamping to produce samples for single lap shear analysis. The formulation based on HMM was applied as soon as it became homogeneous, whereas the HMMM formulation included 30 vol.% water and was used immediately after mixing. Force was applied parallel to the slide alignment and the cured slides were pulled apart until either adhesive or substrate failure.

Both HMM and HMMM-based networks (HMM-net and HMMM-net) were tested and compared to several commercial adhesives (Loctite® Glass Glue, Gorilla Glue® Clear, and Gorilla® Max Strength Construction Adhesive Clear) designed for use with glass (Figure 4a). HMM-net demonstrated the highest lap shear capacity and typically resulted in substrate failure before failure of the adhesive (Figure 4b). This performance was comparable to both Gorilla Glue® (GG) samples, which also resulted in substrate failure. HMMM-net, in contrast, was on par with the commercial Loctite samples but showed signs of adhesive failure to the substrate as opposed to cohesive failure of the sample. This difference in performance could be attributed to processing conditions and rates of polymerization. In the case of HMM-net, when it is applied at room temperature, polymerization within the sample may be slow enough to have some surface interaction with the glass. However, HMMM could be condensing with BTMSEB too quickly within the solution to form network-substrate bonds.

In addition to being remarkably strong, smaller quantities of HMM-net were required to achieve adhesion compared to the commercial adhesives (Table S2). The thickness at the lap shear joint was recorded after curing to determine the height of the adhesive layer. HMM-net and HMMM-net typically added negligible thickness, similar to Loctite®, whereas the Gorilla Glue® Clear and Max Strength samples required more adhesive, increasing the total thickness by 0.02 and 0.20 mm,

respectively. Minimizing the amount of adhesive material in a joint can be important in structural applications to reduce the weight of adhered parts and maximize space efficiency.[41]

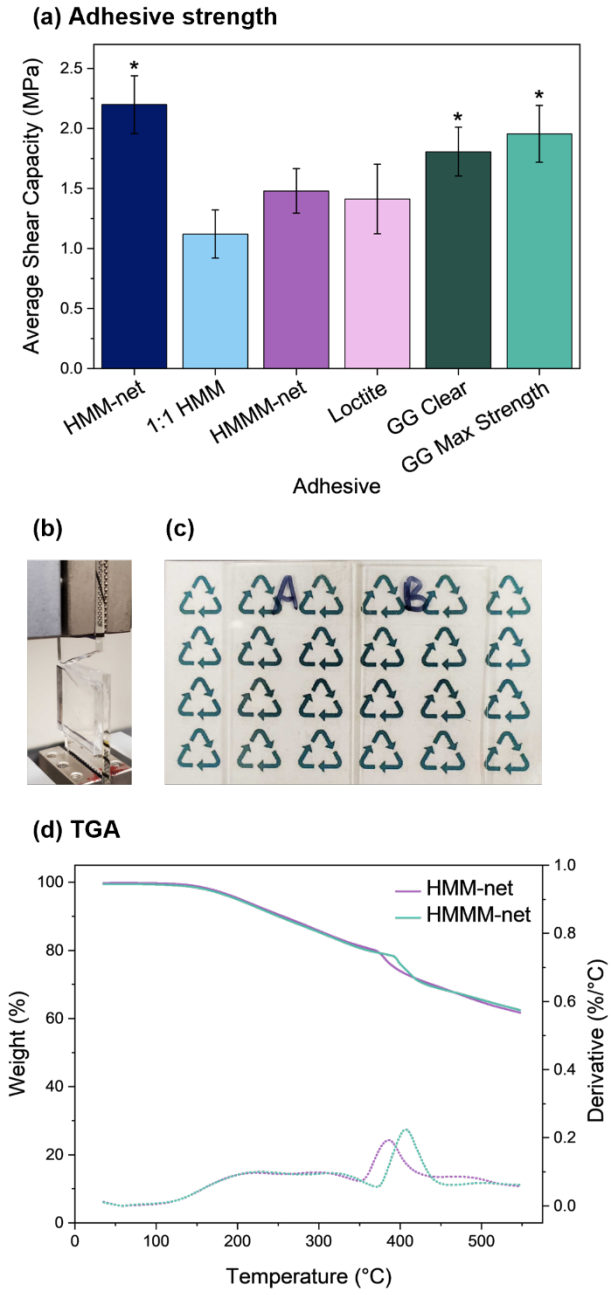

Figure 4. (a) Lap shear capacity as determined by single lap joint adhesion tests. Asterisks indicate that substrate failure was observed. (b) Example of substrate failure from HMM-net samples. (c)

Prepared glass slides coated with HMM-net (A) and HMMM-net (B). (d) TGA of HMM-net and HMMM-net plotted with the first derivative (dotted line).

Another remarkable quality of our thermoset was its transparency. To test its potential as a glass coating, samples were applied as a liquid and drawn across the slide to form a thin layer. These samples were cured at room temperature and formed a thin, clear layer (Figure 4c). The glass slides were affixed to the aperture of an integrating sphere to test the transparency. We observed no significant difference in transmission between the coated and uncoated slides in the visible range (Figure S18).

We also explored the thermal properties of our networks to establish their stability. Thermogravimetric analysis (TGA) of the networks showed good thermal stability with a decomposition temperature at 5% weight loss ($T_{d,5\%}$) near 200 °C for both HMM-net and HMMM-net (Figure 4d). Even with a second thermal decomposition over 350 °C (corresponding to the degradation of the triazine ring), the materials maintained a char mass of over 50% even after an isothermal period of 10 minutes at 550 °C. This high char mass can be attributed to the stability of the aromatic components, which has previously been credited with fire-retardant properties. Differential scanning calorimetry (DSC) was used to probe the glass transition of the network between 25 °C and the onset of degradation at 150 °C but showed no thermal events in that range (Figure S2). Dynamic networks are often mechanically reprocessed if there is enough segmental motion. However, the glass transition temperature of our system was too high to use this method of reprocessing without significant degradation.

3.3 Degradation

3.3.1 Monomer Recovery

Since free alcohol groups are known to exchange with silyl ether bonds in polymer networks,[25] we predicted that exchange with an alcohol solvent could be used to recover the starting materials or other useful small-molecule products. We tried soaking HMM-net in a range of alcohols with varying sterics and polarity, from methanol to butanol and ethylene glycol. All of the alcohols resulted in similar or higher gel fractions at room temperature compared to methanol, which had a gel fraction of 98%. Since HMMM can be synthesized from HMM using excess methanol (see preparation in SI), we moved forward with methanol as the preferred solvent for degradation.[13] Soaking the samples at room temperature for as long as 6 days showed no significant changes in gel fraction, nor did the addition of more catalyst (Table S1). Performing solvolysis at increased temperatures lowered the gel fraction to 94% at 60 ºC for 72 hours and 70% at 90 ºC for 48 hours (in a pressure vessel). Degradation in 90 ºC methanol was monitored over time from 30 minutes to 6 days (Figure 5a). The remaining solid film was dried thoroughly and used to calculate the gel fraction. The methanol solution was filtered to remove any stray solids and collected as the sol fraction. The volatiles were then removed *in vacuo* and the mass of the residue was recorded as the sol fraction. The sol fractions were redissolved in deuterated solvent and analyzed by NMR to identify the products. These spectra indicated the majority soluble product was HMMM, with side products increasing at later timepoints (Figure S19). Surprisingly, there was no sign of alkoxysilane products in the sol fraction.

The combined sol and gel fractions typically accounted for the initial sample mass. However, while the gel fraction began to level off after 24 hours, the total mass recovery decreased. Concomitantly, for dissolution beyond 1 day at 90 ºC, we observed formation of a clear film at the solvent level. This new solid was collected during the filtration of the sol fraction, dried, and its mass was measured. Gratifyingly, this material completed the mass balance for those experiments.

Therefore, mass recovery is maximized and side products are minimized if the degradation is stopped between 12 and 24 hours. However, due to the lack of alkoxysilane recovery in the sol fraction, a more thorough analysis of the insoluble products from degradation was necessary.

We used X-ray photoelectron spectroscopy (XPS) to analyze the elemental composition of the film before and after degradation, as well as the new solid that was collected from the sol fraction. The initial film composition matches what would be expected based upon the formulation of our networks (Figure 5b). The gel fraction showed an increase in the percent composition of silicon relative to the total count after degradation. The new solid showed only trace amounts of Si in the composition. We therefore propose that the triazine elements are selectively removed from the network via methanolysis, while the silyl ether network remains intact. Despite nearly 75% of the material remaining as a solid, HMM makes up 28% of the initial film by weight, indicating that a high recovery of the triazine component is achieved. By adjusting the formulation to 1:1 HMM:BTMSEB (44 wt% HMM), we recover a sol fraction of 46%, but still do not see any alkoxysilane in the sol fraction by NMR. The 1:1 formulation is unfortunately accompanied by a decrease in adhesive properties, suggesting that selection of an appropriate formulation should take into consideration the relative importance of strength *vs*. degradability (Figure 4a, Table S2).

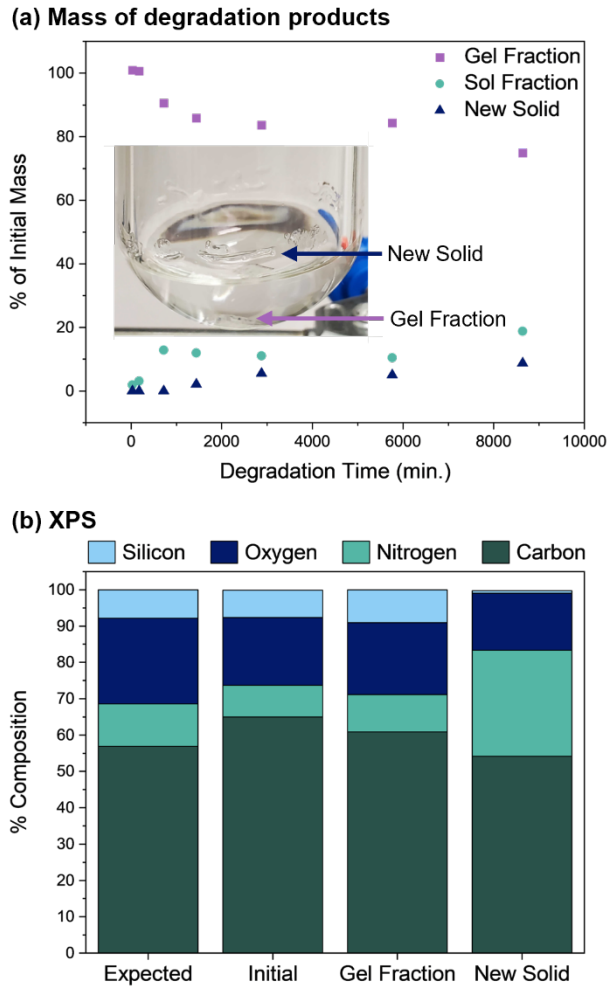

Figure 5. (a) Mass balance of methanolysis procedure (75 mg HMM-net in 10 mL MeOH at 90 °C) over time with an inset presenting the different fractions that were measured. (b) Elemental composition of various components in the degradation experiment based on XPS survey scans.

These observations indicated that any remaining network would be composed mainly of Si–O bonds, so we tried harsher conditions to further break down HMM-net. A 1 M solution of tetrabutylammonium fluoride (TBAF) in THF did not show any significant degradation of the material, but 24 hours in a 70% hydrofluoric acid solution in pyridine resulted in 42% mass loss. Given the hazards associated with handling concentrated HF, we did not explore this pathway

further, but have proven that further degradation is possible through conditions aside from methanolysis.

3.3.2 Adhesive Degradation

To demonstrate the advantage of dynamic bonds in our network, single lap shear samples were soaked in 60 °C methanol overnight before being tested for adhesive strength. The degraded HMM-net samples (HMM-deg) could not be loaded into the clamps of the instrument before showing cohesive failure (Table S2). Degraded HMMM-net (HMMM-deg), on the other hand, produced inconsistent results. Most samples broke while loading while others showed only a minimal decrease in strength, limiting the circularity of these degradable materials. These differences could be attributed to differences in processing conditions, reaction kinetics, or network connectivity. One possible explanation for the resistance of HMMM-net adhesives to methanolysis is greater formation of homo-coupled silyl ether oligomers, which are not degraded under these conditions. This conclusion is supported by a comparison of FTIR of the gel fractions from the degraded networks. HMMM-deg shows more evidence of Si–O bonding than either HMM-deg or HMMM-net (Figure S1). Changes in the rate of gelation could also affect how the networks bind to the surface. All of the HMMM-net and HMMM-deg samples displayed adhesive failure, indicating preferential binding to one of the glass slides. Therefore, lap shear adhesion tests of the HMMM-based adhesives may be more indicative of the strength of the substrate–network bond as opposed to the strength of the internal chemical bonds. If adhesive failure is contributing to the maximum force applied during the lap shear tests, the effects of degradation on network strength could be less pronounced.

4. Conclusions

We have demonstrated ultra-strong, transparent, and degradable adhesives can be derived from both HMM and HMMM in tandem with alkoxysilanes. Our proposed mechanism involves the attack of silanol crosslinker on an iminium ion that is formed by either triazine in the presence of acid catalyst. The silyl ether bonds in the network add dynamicity that can be used to solvolyze the network, freeing the triazine component. These thermosets can achieve glass adhesion that is competitive with commercial products while requiring less material. The transparency of the cured network makes it even more desirable for use with transparent materials like glass. Solvolysis allows recovery of both the glass substrates and HMMM, which can be re-used as a rubber additive, flame retardant, and crosslinker.[16–18] This work contributes to the growing body of materials that combine degradability and performance, and our mechanistic studies revealing the curing mechanism will prove useful in expanding the scope of sustainable polymer networks.

Supporting Information.

The following files are available free of charge.

Supporting Information includes experimental procedures; sample preparation; NMR; FTIR; UV/Vis/NIR; gel fractions; rheology; computations; and XPS. (PDF)

The primary data associated with this study are openly available in Northwestern University's digital repository, Arch, at https://doi.org/10.21985/n2-qgvx-es42.

Corresponding Author

*Julia A. Kalow – Department of Chemistry, Northwestern University, Evanston, Illinois 60208, United States

Email: jkalow@northwestern.edu

Present Addresses

Ian C. Pierce – Department of Chemistry, Northwestern University, Evanston, Illinois 60208, United States

Jorge Barroso – Department of Chemistry, The University of South Dakota, Vermillion, South Dakota 57069, United States

†Department of Chemistry, Clemson University, Clemson, South Carolina 29634, United States

Joanne B. Ko – Department of Chemistry, Northwestern University, Evanston, Illinois 60208, United States

Bess Vlaisavljevich – Department of Chemistry, The University of South Dakota, Vermillion, South Dakota 57069, United States

Author Contributions

The manuscript was written through contributions of all authors. All authors have given approval to the final version of the manuscript.

Notes

The authors declare no competing financial interest.

Acknowledgements

This research was supported by funding from the NSF Center for Sustainable Polymers (CSP) (CHE-1901635). This work made use of equipment funded by the Soft and Hybrid Nanotechnology Experimental (ShyNE) Resource (NSF ECCS-2025633), Northwestern's MRSEC program (NSF DMR-2308691), and the NCI Cancer Center Support Grant (#P30

CA060553) which help fund the Integrated Materials Structure Education and Research Center (IMSERC), Keck-II facility of the NUANCE Center, and the Keck Biophysics, MatCI, and CLaMMP facilities, with additional support from the State of Illinois and the International Institute for Nanotechnology (IIN). The authors would also like to thank Erin Maines and the Ellison group at the University of Minnesota for useful discussions regarding characterization.

References

(1) Biron, M. 2 - The Plastics Industry: Economic Overview. In *Thermosets and Composites (Second Edition)*; Biron, M., Ed.; William Andrew Publishing: Oxford, 2014; pp 25–104. https://doi.org/10.1016/B978-1-4557-3124-4.00002-X.

(2) Post, W.; Susa, A.; Blaauw, R.; Molenveld, K.; Knoop, R. J. I. A Review on the Potential and Limitations of Recyclable Thermosets for Structural Applications. *Polym. Rev.* 2020, *60* (2), 359–388. https://doi.org/10.1080/15583724.2019.1673406.

(3) Crews, G. M.; Ripperger, W.; Kersebohm, D. B.; Güthner, T.; Mertschenk, B. Melamine and Guanamines. In *Ullmann's Encyclopedia of Industrial Chemistry*; Wiley-VCH, Ed.; Wiley, 2006. https://doi.org/10.1002/14356007.a16_171.pub2.

(4) Ma, X.-X.; Wu, Y.-Z.; Zhu, H.-L. The Fire-Retardant Properties of the Melamine-Modified Urea–Formaldehyde Resins Mixed with Ammonium Polyphosphate. *J. Wood Sci.* 2013, *59* (5), 419–425. https://doi.org/10.1007/s10086-013-1350-6.

(5) Shan, H.; Yan, L.; Xu, B.; Wang, D.; Wu, M. Polyphosphamide Containing Triazine and Melamine Cyanurate for Flame-Retardant PA6. *ACS Appl. Polym. Mater.* 2023, *5* (7), 5322–5333. https://doi.org/10.1021/acsapm.3c00732.

(6) Binder, W. H.; Dunky, M. Melamine-Formaldehyde Resins. In *Encyclopedia of polymer science and technology*; Mark, H. F., Ed.; Wiley-Interscience: Hoboken, N.J, 2007; pp 654–657.

(7) Pizzi, A. Melamine-Formaldehyde Adhesives. In *Handbook of Adhesive Technology, Revised and Expanded*; CRC Press, 2003; pp 636–663.

(8) Stamm, A. J.; Seborg, R. M. Minimizing Wood Shrinkage and Swelling: Treating with Synthetic Resin-Forming Materials. *Ind. Eng. Chem.* 1936, *28* (10), 1164–1169. https://doi.org/10.1021/ie50322a009.

(9) Young No, B.; Kim, M. G. Evaluation of Melamine-Modified Urea-Formaldehyde Resins as Particleboard Binders. *J. Appl. Polym. Sci.* 2007, *106* (6), 4148–4156. https://doi.org/10.1002/app.26770.

(10) Kandelbauer, A.; Petek, P.; Medved, S.; Pizzi, A. P.; Teischinger, A. On the Performance of a Melamine–Urea–Formaldehyde Resin for Decorative Paper Coatings. *Eur. J. Wood Wood Prod.* 2009, *68*, 63–75. https://doi.org/10.1007/s00107-009-0352-y.

(11) Merline, D. J.; Vukusic, S.; Abdala, A. A. Melamine Formaldehyde: Curing Studies and Reaction Mechanism. *Polym. J.* 2013, *45* (4), 413–419. https://doi.org/10.1038/pj.2012.162.

(12) Tomita, B. Melamine–Formaldehyde Resins: Molecular Species Distributions of Methylolmelamines and Some Kinetics of Methylolation. *J. Polym. Sci. Polym. Chem. Ed.* 1977, *15* (10), 2347–2365. https://doi.org/10.1002/pol.1977.170151005.

(13) Wang, H. Inorganic Hybridized Methanol Etherified Melamine Resin and Preparation Method Thereof. CN106349268A, January 25, 2017.

(14) Hong, X.; Chen, Q.; Chen, M.; Chen, J.; Liu, H. A Novel Coating by Hybrid Polymerization. *Prog. Org. Coat.* 2002, *45* (2), 165–171. https://doi.org/10.1016/S0300-9440(02)00044-9.

(15) Saxon, R.; Lestienne, F. C. Curing Relations of Hexakis(Methoxymethyl)Melamine and Its Combinations with Acrylic Polymers. *J. Appl. Polym. Sci.* 1964, *8* (1), 475–488. https://doi.org/10.1002/app.1964.070080131.

(16) Xiong, Z.; Chen, N.; Wang, Q. Fabrication and Characterization of Melamine Formaldehyde Fibers with Enhanced Mechanical Properties and High Fire Resistance by Dry Spinning. *J. Appl. Polym. Sci.* 2020, *137* (45), 49385. https://doi.org/10.1002/app.49385.

(17) Sorce, F. S.; Shields, T.; Ngo, S.; Lowe, C.; Taylor, A. C. The Effect of Varying Molecular Weight on the Performance of HMMM-Crosslinked Polyester Coatings. *Prog. Org. Coat.* 2020, *149*, 105920. https://doi.org/10.1016/j.porgcoat.2020.105920.

(18) Dhanalakshmi, J.; Vijayakumar, C. T. Thermal Studies on Dry Bonding Adhesive System for Potential Rubber Article Applications. *J. Adhes. Sci. Technol.* 2020, *34* (3), 233–245. https://doi.org/10.1080/01694243.2019.1663700.

(19) Zheng, N.; Xu, Y.; Zhao, Q.; Xie, T. Dynamic Covalent Polymer Networks: A Molecular Platform for Designing Functions beyond Chemical Recycling and Self-Healing. *Chem. Rev.* 2021, *121* (3), 1716–1745. https://doi.org/10.1021/acs.chemrev.0c00938.

(20) Shieh, P.; Zhang, W.; Husted, K. E. L.; Kristufek, S. L.; Xiong, B.; Lundberg, D. J.; Lem, J.; Veysset, D.; Sun, Y.; Nelson, K. A.; Plata, D. L.; Johnson, J. A. Cleavable Comonomers Enable

Degradable, Recyclable Thermoset Plastics. *Nature* 2020, *583* (7817), 542–547. https://doi.org/10.1038/s41586-020-2495-2.

(21) Gormong, E. A.; Sneddon, D. S.; Reineke, T. M.; Hoye, T. R. Neighboring Group Effects on the Rates of Cleavage of Si–O–Si-Containing Compounds. *J. Org. Chem.* 2023, *88* (4), 1988–1995. https://doi.org/10.1021/acs.joc.2c02126.

(22) Johnson, A. M.; Johnson, J. A. Thermally Robust yet Deconstructable and Chemically Recyclable High-Density Polyethylene (HDPE)-Like Materials Based on Si–O Bonds. *Angew. Chem. Int. Ed.* 2023, *62* (51), e202315085. https://doi.org/10.1002/anie.202315085.

(23) Osthoff, R. C.; Bueche, A. M.; Grubb, W. T. Chemical Stress-Relaxation of Polydimethylsiloxane Elastomers. *J. Am. Chem. Soc.* 1954, *76* (18), 4659–4663. https://doi.org/10.1021/ja01647a052.

(24) Zheng, P.; McCarthy, T. J. A Surprise from 1954: Siloxane Equilibration Is a Simple, Robust, and Obvious Polymer Self-Healing Mechanism. *J. Am. Chem. Soc.* 2012, *134* (4), 2024–2027. https://doi.org/10.1021/ja2113257.

(25) Nishimura, Y.; Chung, J.; Muradyan, H.; Guan, Z. Silyl Ether as a Robust and Thermally Stable Dynamic Covalent Motif for Malleable Polymer Design. *J. Am. Chem. Soc.* 2017, *139* (42), 14881–14884. https://doi.org/10.1021/jacs.7b08826.

(26) Tretbar, C. A.; Neal, J. A.; Guan, Z. Direct Silyl Ether Metathesis for Vitrimers with Exceptional Thermal Stability. *J. Am. Chem. Soc.* 2019, *141* (42), 16595–16599. https://doi.org/10.1021/jacs.9b08876.

(27) Husted, K. E. L.; Brown, C. M.; Shieh, P.; Kevlishvili, I.; Kristufek, S. L.; Zafar, H.; Accardo, J. V.; Cooper, J. C.; Klausen, R. S.; Kulik, H. J.; Moore, J. S.; Sottos, N. R.; Kalow, J. A.; Johnson, J. A. Remolding and Deconstruction of Industrial Thermosets via Carboxylic Acid-Catalyzed Bifunctional Silyl Ether Exchange. *J. Am. Chem. Soc.* 2023, *145* (3), 1916–1923. https://doi.org/10.1021/jacs.2c11858.

(28) Hsiue, G.-H.; Lee, R.-H.; Jeng, R.-J. A New Class of Organic–Inorganic Sol–Gel Materials for Second-Order Nonlinear Optics. *Chem. Mater.* 1997, *9* (4), 883–888. https://doi.org/10.1021/cm960445f.

(29) Tamami, B.; Betrabet, C.; Wilkes, G. L. New Ceramer High Optical Abrasion Resistant Transparent Coating Materials Based on Functionalized Melamine and a Tris(m-Aminophenyl)Phosphine Oxide Compound. *Polym. Bull.* 1993, *30* (1), 39–45. https://doi.org/10.1007/BF00296232.

(30) Chen, J.-I.; Chareonsak, R.; Puengpipat, V.; Marturunkakul, S. Organic/Inorganic Composite Materials for Coating Applications. *J. Appl. Polym. Sci.* 1999, *74* (6), 1341–1346. https://doi.org/10.1002/(SICI)1097-4628(19991107)74:6<1341::AID-APP3>3.0.CO;2-4.

(31) Urdl, K.; Weiss, S.; Karpa, A.; Perić, M.; Zikulnig-Rusch, E.; Brecht, M.; Kandelbauer, A.; Müller, U.; Kern, W. Furan-Functionalised Melamine-Formaldehyde Particles Performing Diels-Alder Reactions. *Eur. Polym. J.* 2018, *108*, 225–234. https://doi.org/10.1016/j.eurpolymj.2018.08.023.

(32) Urdl, K.; Weiss, S.; Brodbeck, B.; Kandelbauer, A.; Zikulnig-Rusch, E.; Müller, U.; Kern, W. Homogeneous, Monodispersed Furan-Melamine Particles Performing Reversible Binding and

Forming Networks. *Eur. Polym. J.* 2019, *116*, 158–168. https://doi.org/10.1016/j.eurpolymj.2019.04.006.

(33) Urdl, K.; Weiss, S.; Christöfl, P.; Kandelbauer, A.; Müller, U.; Kern, W. Diels-Alder Modified Self-Healing Melamine Resin. *Eur. Polym. J.* 2020, *127*, 109601. https://doi.org/10.1016/j.eurpolymj.2020.109601.

(34) Lei, Z.; Chen, H.; Luo, C.; Rong, Y.; Hu, Y.; Jin, Y.; Long, R.; Yu, K.; Zhang, W. Recyclable and Malleable Thermosets Enabled by Activating Dormant Dynamic Linkages. *Nat. Chem.* 2022, *14* (12), 1399–1404. https://doi.org/10.1038/s41557-022-01046-4.

(35) Smith, K. A. Polycondensation of Methyltrimethoxysilane. *Macromolecules* 1987, *20* (10), 2514–2520. https://doi.org/10.1021/ma00176a033.

(36) Blank, W. J. Reaction Mechanism of Melamine Resins. *J. Coat. Technol.* 1979, *51* (656), 61–70.

(37) Wang, H.; Li, X.; Zhang, E.; Shi, J.; Xiong, X.; Kong, C.; Ren, J.; Li, C.; Wu, K. Strong Thermo-Tolerant Silicone-Modified Waterborne Polyurethane/Polyimide Pressure-Sensitive Adhesive. *Langmuir* 2023, *39* (49), 17611–17621. https://doi.org/10.1021/acs.langmuir.3c01564.

(38) Weiss, S.; Urdl, K.; Mayer, H. A.; Zikulnig-Rusch, E. M.; Kandelbauer, A. IR Spectroscopy: Suitable Method for Determination of Curing Degree and Crosslinking Type in Melamine–Formaldehyde Resins. *J. Appl. Polym. Sci.* 2019, *136* (25), 47691. https://doi.org/10.1002/app.47691.

(39) Parr, R. G.; Yang, W. Density Functional Approach to the Frontier-Electron Theory of Chemical Reactivity. *J. Am. Chem. Soc.* 1984, *106* (14), 4049–4050. https://doi.org/10.1021/ja00326a036.

(40) Wang, B.; Rong, C.; Chattaraj, P. K.; Liu, S. A Comparative Study to Predict Regioselectivity, Electrophilicity and Nucleophilicity with Fukui Function and Hirshfeld Charge. *Theor. Chem. Acc.* 2019, *138* (12), 124. https://doi.org/10.1007/s00214-019-2515-1.

(41) Arenas, J. M.; Narbón, J. J.; Alía, C. Optimum Adhesive Thickness in Structural Adhesives Joints Using Statistical Techniques Based on Weibull Distribution. *Int. J. Adhes. Adhes.* 2010, *30* (3), 160–165. https://doi.org/10.1016/j.ijadhadh.2009.12.003.

For Table of Contents Only